

Diabatization based on the dipole and quadrupole: The DQ method

Chad E. Hoyer, Xuefei Xu, Dongxia Ma, Laura Gagliardi, and Donald G. Truhlar

Citation: *The Journal of Chemical Physics* **141**, 114104 (2014); doi: 10.1063/1.4894472

View online: <http://dx.doi.org/10.1063/1.4894472>

View Table of Contents: <http://scitation.aip.org/content/aip/journal/jcp/141/11?ver=pdfcov>

Published by the [AIP Publishing](#)

Articles you may be interested in

Quadrupole, octopole, and hexadecapole electric moments of π , σ , and δ electronic states: Cylindrically asymmetric charge density distributions in linear molecules with nonzero electronic angular momentum
J. Chem. Phys. **127**, 074107 (2007); 10.1063/1.2755691

Time-dependent approach to electronically excited states of molecules with the multiconfiguration time-dependent Hartree-Fock method
J. Chem. Phys. **126**, 214106 (2007); 10.1063/1.2743007

Dipole and quadrupole moments of molecules in crystals: A novel approach based on integration over Hirshfeld surfaces
J. Chem. Phys. **124**, 074106 (2006); 10.1063/1.2173990

First-principle molecular dynamics with ultrasoft pseudopotentials: Parallel implementation and application to extended bioinorganic systems
J. Chem. Phys. **120**, 5903 (2004); 10.1063/1.1652017

Determining the molecular Aharonov–Bohm phase angle: A rigorous approach employing a molecular properties based adiabatic to diabatic states transformation
J. Chem. Phys. **110**, 701 (1999); 10.1063/1.477917



COMSOL
CONFERENCE
2014 BOSTON

The Multiphysics
Simulation
Event of the Year



LEARN MORE >>

Diabatization based on the dipole and quadrupole: The DQ method

Chad E. Hoyer, Xuefei Xu, Dongxia Ma, Laura Gagliardi,^{a)} and Donald G. Truhlar^{a)}

Department of Chemistry, Chemical Theory Center, and Supercomputing Institute, University of Minnesota, 207 Pleasant St. SE, Minneapolis, Minnesota 55455-0431, USA

(Received 26 June 2014; accepted 21 August 2014; published online 15 September 2014)

In this work, we present a method, called the DQ scheme (where D and Q stand for dipole and quadrupole, respectively), for transforming a set of adiabatic electronic states to diabatic states by using the dipole and quadrupole moments to determine the transformation coefficients. It is more broadly applicable than methods based only on the dipole moment; for example, it is not restricted to electron transfer reactions, and it works with any electronic structure method and for molecules with and without symmetry, and it is convenient in not requiring orbital transformations. We illustrate this method by prototype applications to two cases, LiH and phenol, for which we compare the results to those obtained by the fourfold-way diabatization scheme. © 2014 AIP Publishing LLC. [<http://dx.doi.org/10.1063/1.4894472>]

I. INTRODUCTION

The Born-Oppenheimer approximation separates the electronic and nuclear motion, and this separation leads to electronically adiabatic states and potential energy surfaces (PESs); approximations to the electronically adiabatic states may be obtained by the standard electronic structure methods. Nuclear motion couples the adiabatic states through the nuclear momentum. Obtaining analytical representations of potential energy surfaces and couplings in the adiabatic representation is difficult because the states and surfaces have discontinuous first derivatives, and the momentum couplings have singularities. This motivates transforming to another representation. One might at first hope to transform to a representation with smooth surfaces and zero momentum couplings. However, such a representation does not in general exist.¹ However, one can find representations with smooth surfaces and negligible momentum couplings, and a representation with this property is called diabatic.² Diabatic states do not diagonalize the electronic Hamiltonian, and so they are coupled by off-diagonal elements of the electronic Hamiltonian operator. They are not unique, and a variety of approaches to obtaining diabatic states have been proposed, although many of them are not general. A general feature of diabatic states is that they should be smooth functions of nuclear coordinates since the nuclear momentum operator involves derivatives with respect to nuclear coordinates, and these will not be negligible if the state functions are not smooth and slowly varying. In the present article, we propose a new way to obtain diabatic states and we compare it to previous work. We limit ourselves to methods in which diabatic states are defined as linear combinations of the same number of adiabatic states. We propose a general procedure in which we use standard electronic structure methods to obtain a set of low-energy adiabatic states and then transform them to a diabatic basis that spans the same space.

In general, the specification of electronic states requires first defining an orbital basis, then defining many-electron functions (usually called configuration state functions or CSFs) in terms of these orbitals, and then specifying the states as linear combinations of the CSFs. We note that the orbitals and CSFs are not physical observables. One way to construct diabatic states is to rotate the adiabatic states in such a way as to directly minimize the nuclear-momentum couplings. This way involves directly computing the couplings, which is cumbersome because they are $(3N - 6)$ -dimensional vectors that depend on electronic origin,³⁻⁵ do not necessarily vanish upon atomization,^{2,6} and are singular on $(3N - 8)$ -dimensional surfaces,⁷ where N is the number of atoms.

Another approach is transforming the adiabatic states to states that are smooth functions of the internuclear coordinates.⁸⁻²¹ Probably, the most straightforward way to do this is to define smoothly varying orbitals (which may be called diabatic molecular orbitals or DMOs) in terms of which one may define smoothly varying CSFs to be used to define the state functions, as is done in the configurational uniformity method of Atchity and Ruedenberg^{11,12} and in the fourfold way,¹⁵⁻¹⁸ whose final step is configurational uniformity. Many methods for enforcing smoothness depend on following a path through configuration space, for example, by enforcing high overlap with the diabatic states at the previous point in space¹⁹ or by maximizing some function of the overlap of the orbitals;^{20,21} even for triatomic systems that have only three internal coordinates, this becomes cumbersome if one wants to generate a full potential energy surfaces, and for four or more atoms, it becomes impractical. Methods that allow the direct generation of diabatic states at a given geometry are called direct diabatization and are preferred for this reason.

A third approach is to define diabatic states by using physical observables without defining DMOs. Of the observables one could choose, the dipole moment has received much attention both historically and recently,²²⁻³¹ but we will show that it is much more robust to use both the dipole moment and the quadrupole moment. The historical context of these methods will be discussed in Sec. II.

^{a)} Authors to whom correspondence should be addressed. Electronic addresses: gagliardi@umn.edu and truhlar@umn.edu.

Our motivation for using information about the quadrupole moment in addition to the dipole was to develop a diabaticization method that is more generally applicable than schemes based only on the dipole. The dipole locates the center of charge (first moment of the charge distribution), which is important for charge transfer reactions, but the quadrupole moment provides information about the shape of the charge distribution that is more general and can extend the applicability to photochemical reactions that are not classifiable as charge transfer processes. In Sec. II, in addition to providing historical context, we will review the fourfold way^{15–18} and Boys localization²⁸ methods for diabaticization before discussing the new method, which we call the DQ method, where D and Q stand for dipole and quadrupole, respectively. The fourfold way, the Boys localization method, and the DQ method are all direct; but the fourfold way requires orbital transformations, whereas Boys localization and the DQ method do not, which is more convenient and requires less programming to extend the method to arbitrary electronic structure methods. In Secs. III and IV, we will provide computational details and results of these three methods applied to two cases: LiH and phenol.

II. THEORY

II.A. Notation

In this article, we only consider diabaticization methods in which N diabatic states span the same space as N selected adiabatic states, which may be (but need not necessarily be) the N lowest-energy adiabatic states. Given N adiabatic states, $\{\psi_I\}$, we express diabatic states, $\{\phi_A\}$, as a linear combination of these N states

$$\phi_A = \sum_{I=1}^N \psi_I T_{IA}, \quad I = 1, \dots, N. \quad (1)$$

The diabatic energy matrix, \mathbf{U} , is computed from the adiabatic energy matrix, \mathbf{V} , as

$$U_{AB} = \sum_I T_{IA} V_I T_{IB}, \quad (2)$$

where the transformation matrix \mathbf{T} depends on the diabaticization method used.

II.B. Review of the fourfold way

The fourfold way^{15–18} is a general diabaticization scheme based on configurational uniformity¹² and is currently available for transforming complete-active-space self-consistent field (CASSCF)³² adiabatic states or multiconfiguration quasidegenerate perturbation theory (MC-QDPT) adiabatic states obtained with a CASSCF reference wave function.³³ It has been presented previously^{15–18} and applied successfully to a number of problems.^{34–40} We will also apply it here for comparison with the new DQ method. In this section, we review the key elements of the fourfold way. To enforce configurational uniformity, the adiabatic states need to be written as a linear combination of CSFs expressed in terms of DMOs, and one must choose diabatic prototype states; then the elec-

tronic states are transformed to have maximum resemblance to the diabatic prototype states. Thus, there are two transformations involved, in particular an orbital transformation to yield DMOs and a CSF transformation to yield diabatic states.

The generation of smooth DMOs is the key feature of the fourfold way method. The DMOs of the inactive and virtual orbitals are assumed to be equivalent to the canonical MOs from the CASSCF calculations, and those for the active space are obtained by rotating the active MOs in a systematic way by a scheme called the fourfold way, which generates DMOs by satisfying the threefold-density-matrix criterion and, if needed, the maximum-overlap-reference-MOs (MORMO) criterion, which is the fourth element.

The threefold-density-matrix criterion is satisfied by maximizing a three-term functional

$$D_3 = \alpha_N D^{\text{NO}} + \alpha_R D^{\text{ON}} + \alpha_T D^{\text{TD}}, \quad (3)$$

which is a weighted sum of three functionals, where each α is a weight. The three terms are the state-averaged natural orbital term (D^{NO}), the sum of the squares of the orbital occupation numbers for all states (D^{ON}), and a term based on the transition density matrix (D^{TD}). The details and physical motivation for these terms can be found in the original papers.^{15–18} If one generates DMOs from only the threefold-density criterion, which is sometimes sufficient, the method reduces to the threefold way.

The MORMO criterion in the fourfold way is also referred to as the reference-orbital overlap term, D^{RO} , and it is usually needed to resolve degeneracies, for example, in cases involving two or more nonbonding p orbitals on the same center (one or both of these p orbitals might be bonding at some geometries and nonbonding at others, but to obtain global potential energy surfaces we need a global transformation to DMOs, so the transformation must also be valid in regions where both are nonbonding). If reference orbitals are needed, one must first choose λ reference DMOs (where λ is usually 1 or 2) as linear combinations of active orbitals at a reference geometry (\mathbf{R}^{ref}), then determine the λ DMOs at any other geometry \mathbf{R} by maximizing the reference-overlap term⁴¹

$$D^{\text{RO}} = \left| \sum_i \sum_j k_i(\mathbf{R}^{\text{ref}}) k_j(\mathbf{R}) \xi_i(\mathbf{R}) | \xi_j(\mathbf{R}) \right|^2, \quad (4)$$

where $\xi_i(\mathbf{R})$ is an atomic (contracted) basis function at the geometry \mathbf{R} , and k_i is a MO coefficient. The remaining DMOs are generated through the threefold-density-matrix criterion.

It is particularly notable that the fourfold way is not limited to two-center, two-state electron transfer problems, which have been the motivation for many of the diabaticization methods that have been proposed, but rather it is designed to treat more general problems in photochemistry. The fourfold-way diabaticization has been found to work for all systems to which we have tried to apply it.^{15–18,34–40} The main drawback is that the proper choice of reference orbitals and the determination of prototype CSFs for the configurational uniformity step require system-dependent decisions that can be time-consuming and may require expert knowledge of the system at hand. The latter is not entirely unexpected since practical methods involving multiconfiguration reference functions and

excited states usually require system-dependent expertise and often require delicate choices about how to treat the various orbitals.^{42–44}

II.C. Review of the Boys localization diabatization method

In contrast to the fourfold way, which is based mainly on smoothness, one may also base a diabatization scheme on localization.^{25–30} We begin by reviewing the Boys localization scheme developed by Subotnik *et al.*²⁸ because the DQ method may be considered an extension of that scheme. The Boys localization scheme was originally developed for localizing orbitals,^{45,46} and it was extended to the localization of many-electron states by Subotnik *et al.*²⁸ This scheme defines the rotation matrix T of Eq. (1) such that it maximizes the magnitude of the dipole moment difference between diabatic states

$$f_{Boys} = \sum_{A,B} |\langle \phi_A | \boldsymbol{\mu} | \phi_A \rangle - \langle \phi_B | \boldsymbol{\mu} | \phi_B \rangle|^2. \quad (5)$$

This scheme may be motivated by its appropriateness for treating two-state, two-center electron transfer, for which it maximizes the localization of charge on the left in one state (state with the most negative dipole moment) and the localization of charge on the right in the other state (state with maximum positive dipole moment). However, Subotnik and co-workers showed that it is also applicable to more general problems.^{31,47–49} As shown in the Appendix, Eq. (5) is equivalent to maximizing the sum of the squares of the magnitudes of the dipole moments

$$f_{Boys} = \sum_A |\langle \phi_A | \boldsymbol{\mu} | \phi_A \rangle|^2 \equiv \sum_A |\boldsymbol{\mu}_{AA}|^2. \quad (6)$$

The Boys localization scheme is only able to differentiate between electronic states of differing dipole moment. Thus, this method can have difficulty when there are more diabatic states than charge centers. For this reason, it was recommended to rediagonalize any sub-block of the Hamiltonian that corresponds to the same charge center.^{25,28} This is a complicating feature that can be unsatisfactory if the charge accumulation on various centers is a function of geometry; however, the method is still very convenient because it can be used with any electronic structure method and only uses the adiabatic dipole matrix as input without requiring orbital transformations.

To further motivate the use of methods like Boys localization for diabatization, we next discuss the older method of Werner and Meyer.²⁴ In this method, diabatic states are defined as those that satisfy $\langle \phi_A | \boldsymbol{\mu} | \phi_B \rangle = 0$, which are interpreted as charge-localized states. Diagonalizing $\boldsymbol{\mu}$ fulfills this criterion. This method is straightforward and works for more than two states. However, unless the direction of $\boldsymbol{\mu}_{AB}$ is determined by symmetry (in which case we call the axis with a nonzero component the z axis), one cannot diagonalize all components of the dipole vector with the same transformation. Therefore, when there is more than one nonzero component of $\langle \phi_A | \boldsymbol{\mu} | \phi_B \rangle$, the Werner-Meyer method will not work or at least becomes ambiguous (as to which component is to

be diagonalized), and this is a serious shortcoming for application to arbitrary geometries of polyatomic molecules, which prevents the method from being useful for calculating diabatic potential energy surfaces in most cases. The Boys localization scheme for diabatization reduces to the Werner-Meyer method when only one component of $\langle \phi_A | \boldsymbol{\mu} | \phi_B \rangle$ is nonzero by symmetry, but it provides a generalization that does not depend on axis choice for arbitrary geometries of polyatomic molecules.

Another method that may be considered to be a generalization of the Werner-Meyer method is the generalized Mulliken-Hush (GMH) method.²⁵ This method is very similar to the Werner-Meyer method, but instead of diagonalizing the dipole operator along a pre-chosen axis, one diagonalizes $\boldsymbol{\mu} \cdot \boldsymbol{v}$, where

$$\boldsymbol{v} = \frac{\boldsymbol{\mu}_{II} - \boldsymbol{\mu}_{JJ}}{|\boldsymbol{\mu}_{II} - \boldsymbol{\mu}_{JJ}|}, \quad (7)$$

for two states. This method reduces to Werner-Meyer when the direction of \boldsymbol{v} is determined by symmetry but is an improvement over Werner-Meyer because one can now treat states that have more than one nonzero component for $\boldsymbol{\mu}$. However, the choice of \boldsymbol{v} for more than two states is not straightforward and is often not sufficient.²⁶ The GMH method was developed for electron transfer, so rediagonalizing any sub-block of the Hamiltonian that corresponded to multiple diabatic states on the same charge center is recommended as in Boys localization diabatization.

Localization may be considered as maximizing differences in the first moments of the charge distributions of the various states, and more generally we can base diabatization on maximization of other well-defined characteristics of the charge distributions. However, in order to be applied conveniently and unambiguously to all points on an entire potential energy surface, the function to be maximized should be independent of the orientation of the axes. The above analysis should make clear that a key advantage of Boys localization²⁶ over the previous methods is that it uses the magnitude of the dipole moment rather than the dipole moment vector, so there are no difficulties regarding the components of the dipole moment or the choice of axes. Furthermore, it is also directly applicable to more than two states. The magnitude of the dipole moment is a nonlinear function of its components, so an iterative procedure is needed rather than a diagonalization, but that is not an impediment to widespread use. However, as will be shown below, we found that – due to the already mentioned shortcoming that the dipole moment is sometimes insufficient to distinguish diabatic states – Boys diabatization does not always yield useful diabatic states, so we developed a new method that is similar in structure to Boys localization but applicable to more general cases.

II.D. DQ diabatization method

Before introducing the new method, we remind the reader that two possible definitions of the quadrupole moment tensor are in use, the so-called primitive quadrupole moment and the traceless quadrupole moment.^{51–55} In the present article, we will use the primitive quadrupole moment, which is defined

by

$$\mathbf{Q} = \sum_i q_i \mathbf{r}_i \mathbf{r}_i, \quad (8)$$

where the sum is over particles (electrons and nuclei), and q_i is the charge on particle i . The traceless quadrupole moment is obtained by subtracting the trace but will not be used here.

We now define the function to be maximized as

$$\begin{aligned} f_{DQ} &= \sum_A (|\langle \phi_A | \boldsymbol{\mu} | \phi_A \rangle|^2) + \sum_j \alpha_j |\text{tr} \langle \phi_A | \mathbf{Q}^{(j)} | \phi_A \rangle|^2 \\ &\equiv \sum_A \left(|\boldsymbol{\mu}_{AA}|^2 + \sum_j \alpha_j |\text{tr} \mathbf{Q}_{AA}^{(j)}|^2 \right), \end{aligned} \quad (9)$$

where α_j is a parameter (with units, in atomic units, of a_0^{-2} , where $1 a_0 \equiv 1$ bohr), j denotes a choice of origin for the quadrupole integrals, and tr denotes a trace. In this work, we encountered no cases where multiple choices of origin were needed, so we will drop the j after Sec. II. With this formulation, f_{DQ} is invariant to the choice of coordinate system. It is origin dependent if the dipole moment or molecular charge is nonzero. This method maintains many of the desirable features of Boys localization and requires only the dipole moment matrix and the trace-of-the-quadrupole-moment matrix as input. As we show in Sec. IV, this can enable one to avoid *a posteriori* subdiagonalization of the Hamiltonian because the quadrupole is often able to differentiate diabatic states with charge concentrated on the same charge center. Thus, the method is applicable to a more general class of reactions.

II.E. DQ diabaticization for two states

In the case of two adiabatic states, Eq. (1) can be written as

$$\begin{pmatrix} \phi_A \\ \phi_B \end{pmatrix} = \begin{pmatrix} \cos \theta & \sin \theta \\ -\sin \theta & \cos \theta \end{pmatrix} \begin{pmatrix} \psi_I \\ \psi_J \end{pmatrix}. \quad (10)$$

When (10) is plugged into (9), we can rewrite the functional to be maximized in terms of adiabatic matrix elements and θ

$$f_{DQ} = f_{DQ}^a + A + \sqrt{A^2 + B^2} \cos(4(\theta - \gamma)), \quad (11)$$

where

$$\begin{aligned} f_{DQ}^a &= |\boldsymbol{\mu}_{II}|^2 + |\boldsymbol{\mu}_{JJ}|^2 + \sum_j (\alpha_j |\text{tr} \mathbf{Q}_{II}^{(j)}|^2 + \alpha_j |\text{tr} \mathbf{Q}_{JJ}^{(j)}|^2) \\ &\equiv |\boldsymbol{\mu}_{II}|^2 + |\boldsymbol{\mu}_{JJ}|^2 + \sum_j (\alpha_j |M_{II}^{(j)}|^2 + \alpha_j |M_{JJ}^{(j)}|^2), \end{aligned} \quad (12)$$

$$\begin{aligned} A &= -\frac{1}{4} |\boldsymbol{\mu}_{II}|^2 - \frac{1}{4} |\boldsymbol{\mu}_{JJ}|^2 + |\boldsymbol{\mu}_{IJ}|^2 + \frac{1}{2} \boldsymbol{\mu}_{II} \cdot \boldsymbol{\mu}_{JJ} \\ &\quad - \sum_j \left(\frac{\alpha_j}{4} |M_{II}^{(j)}|^2 - \frac{\alpha_j}{4} |M_{JJ}^{(j)}|^2 + \alpha_j |M_{IJ}^{(j)}|^2 \right. \\ &\quad \left. + \frac{\alpha_j}{2} M_{II}^{(j)} M_{JJ}^{(j)} \right), \end{aligned} \quad (13)$$

$$\begin{aligned} B &= \boldsymbol{\mu}_{II} \cdot \boldsymbol{\mu}_{IJ} - \boldsymbol{\mu}_{IJ} \cdot \boldsymbol{\mu}_{JJ} \\ &\quad + \sum_j (\alpha_j M_{II}^{(j)} M_{IJ}^{(j)} - \alpha_j M_{IJ}^{(j)} M_{JJ}^{(j)}), \end{aligned} \quad (14)$$

$$\gamma = \text{Arctan} \left(\frac{-B}{A} \right). \quad (15)$$

Then f_{DQ} will be at a maximum when $\theta = \gamma, \gamma + \frac{1}{2}\pi, \dots$, and γ can be found by solving the nonlinear equation $\frac{\partial f_{DQ}}{\partial \theta} |_{\theta=\gamma} = 0$.

II.F. DQ diabaticization for N states

The DQ method is straightforwardly generalized to the N -state case in precisely the same way as Boys localization.^{28,56}

III. COMPUTATIONAL DETAILS

III.A. LiH

The first three $^1\Sigma^+$ states of LiH were investigated. The three adiabatic potential energy curves (V_j , for $j = 1-3$) were computed by state-averaged CASSCF⁵⁰ averaging over three states (SA(3)-CASSCF) with equal weights for each of the three low-energy states and with the aug-cc-pVTZ^{68(a)} basis set with *Molcas* 7.8.⁵⁷ The wave function was constrained to have C_{2v} spatial symmetry, and calculations were done in the A_1 irreducible representation. The active space consists of two electrons in five orbitals, which nominally correspond to $1s_H$, $2s_{Li}$, and $2p_{Li}$; this active space is denoted as CAS(2,5). As functions of internuclear distance, the Li $2p_x$ and $2p_y$ orbitals change character to H $2p_x$ and H $2p_y$ and have occupation numbers less than 0.005 at all geometries.

We carried out diabaticization by the Boys method, by the DQ method with more than one choice of the parameter α , and by the fourfold way. The dipole matrices needed for Boys localization and the DQ method and the quadrupole matrices needed for the DQ method were computed with the RASSI module⁵⁸ of *Molcas* 7.8.⁵⁷ The origin for the quadrupole moment was taken as the Li atom because an origin on or close to the Li atom is needed upon dissociation in order to differentiate between the state-dependent charge distributions on Li.

In the fourfold-way calculations, the threefold density matrix criterion does not need to be augmented by a reference-orbital overlap term in this case, so the fourfold way reduces to the threefold way for this system. The threefold-way diabaticization was performed in the GAMESS⁶⁴ software package with the 2013 patch. There were only three dominant CSFs, and each constitutes its own diabatic prototype group for the configurational uniformity step.

III.B. Phenol

We applied the DQ diabaticization method to a typical path for phenol photodissociation, and we compare the results to those obtained by the fourfold way. In the same way as in our previous study,^{40,67} the planar ground-state minimum-energy structure of phenol was optimized with C_s symmetry by the

CASSCF method using the aug-cc-pVTZ basis set.⁶⁸ The active space includes 12 active electrons and 11 active orbitals and is denoted as CAS(12,11); the active space consists of three π , three π^* , and one each of σ_{CO} , σ_{OH} , σ_{CO}^* , and σ_{CO}^* , and p_z orbitals (where the p_z orbital is a lone pair orbital on oxygen with the C-1, C-2, and C-3 atoms of the phenyl ring placed in the xy plane). The adiabatic PESs of the three states ($^1\pi\pi$, $^1\pi\pi^*$, and $^1\pi\sigma^*$) were calculated by using the state-averaged CASSCF method with the same weight for each of the three states; this is denoted as SA(3)-CASSCF(12,11). These calculations employed the jul-cc-pVDZ⁶⁹ basis set. The dipole and quadrupole moments needed for DQ calculations were obtained using the RASSI module⁵⁸ of *Molcas* 7.8,⁵⁷ and the origin of the quadrupole moment is the center of nuclear mass of the phenoxy subsystem of phenol. The choice of origin was made due to the delocalized nature of the π orbitals on the phenoxy subsystem.

For comparison, the fourfold-way diabatizations were performed by the *HONDOPLUS.2*⁷⁰ program package at the same level, that is, SA(3)-CASSCF(12,11)/jul-cc-pVDZ. The details of fourfold way applied to phenol can be found in a previous paper,⁴⁰ so we do not repeat those details here.

IV. APPLICATIONS

Boys localization has performed well for a variety of charge-transfer cases.^{28,47-49} A pedagogical test case for the performance of Boys localization is provided by the first four states of square He_4^+ .²⁸ In the adiabatic representation, the charge is delocalized over the molecule, and the first four states are not energetically degenerate. However, upon Boys diabatization, one obtains charge-localized states with degenerate energies. In the present article, we consider two more difficult cases. We employ the Boys localization method without block diagonalization because we want to test the method in the context of polyatomic potential energy curves where block diagonalization at some geometries but not others would produce discontinuous potential energy surfaces.

IV.A. LiH

Ionic-covalent crossings have been widely studied in the alkali hydrides.⁵⁹⁻⁶³ The first three $^1\Sigma^+$ states of LiH consist of two covalent states and one ionic state. The ionic diabatic state has a $1s_{\text{H}}^2$ valence configuration and will be denoted state I. The covalent states have the valence configurations $2s_{\text{Li}}1s_{\text{H}}$ (diabatic state S) and $2p_{\text{Li}}1s_{\text{H}}$ (diabatic state P), respectively.

Figure 1 compares diabatic energies (U_i) of the (a) threefold way, (b) Boys localization, and (c) the DQ Scheme with $\alpha = 0.1 a_0^{-2}$ for the three lowest-energy $^1\Sigma^+$ states of LiH (U_1 corresponds to the I state, U_2 to the S state, and U_3 to the P state). The threefold way results in smooth diabats that nicely agree with the adiabats away from crossings as seen in Figure 1(a). Because of the excellent performance of the threefold way in this case, we use it as the reference for comparison. The Boys localization method unacceptably mixes the S and P states at large Li–H distances and shows non-smooth behavior at small Li–H distances. The DQ method

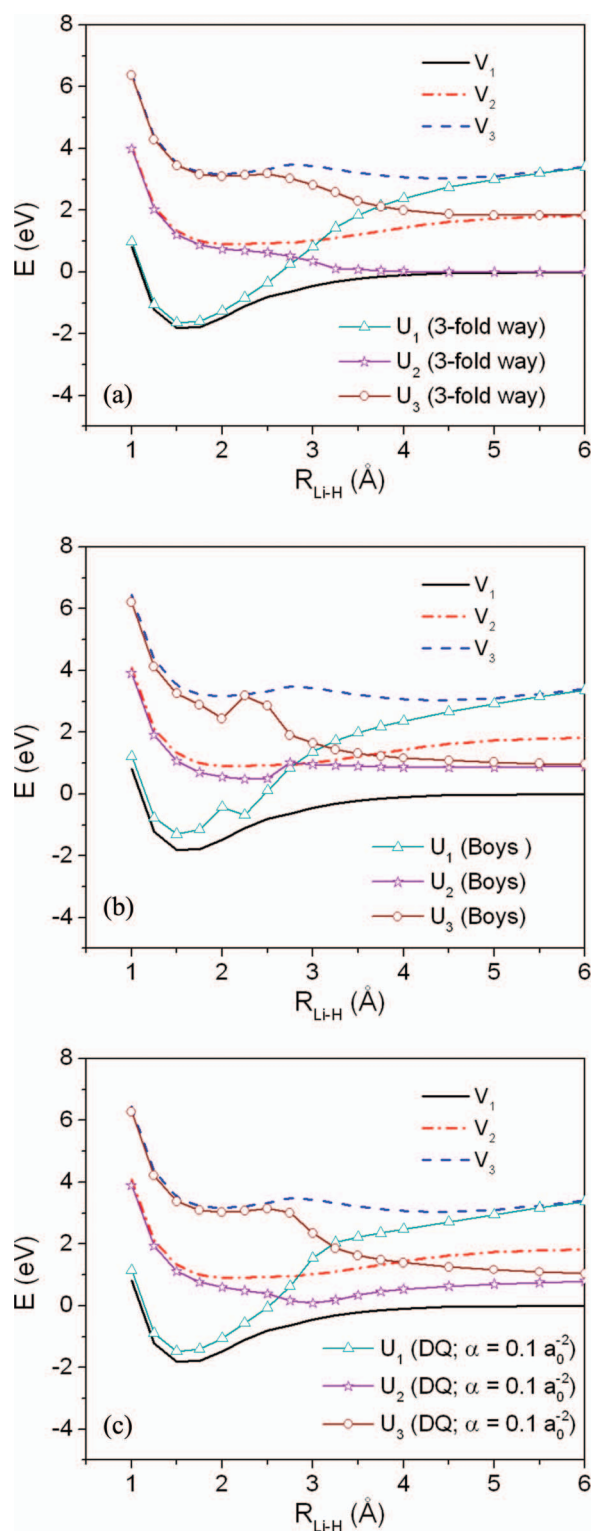


FIG. 1. The adiabatic (V_1 , V_2 , and V_3) and diabatic (U_1 , U_2 , and U_3) potential energy curves of the three lowest-energy $^1\Sigma^+$ states for LiH. The adiabatic states were computed at the SA(3)-CAS(2,5)SCF/aug-cc-pVTZ level of theory and diabatized with (a) the 3-fold way, (b) Boys localization, and (c) the DQ method with $\alpha = 0.1 a_0^{-2}$.

with $\alpha = 0.1 a_0^{-2}$ gives smoother curves than Boys localization but still mixes the S and P states at large Li–H distances. Figure 2(a) shows that the behavior can be fixed for $R_{\text{LiH}} > 4 \text{ \AA}$ by increasing α to $0.5 a_0^{-2}$ but at the cost of making

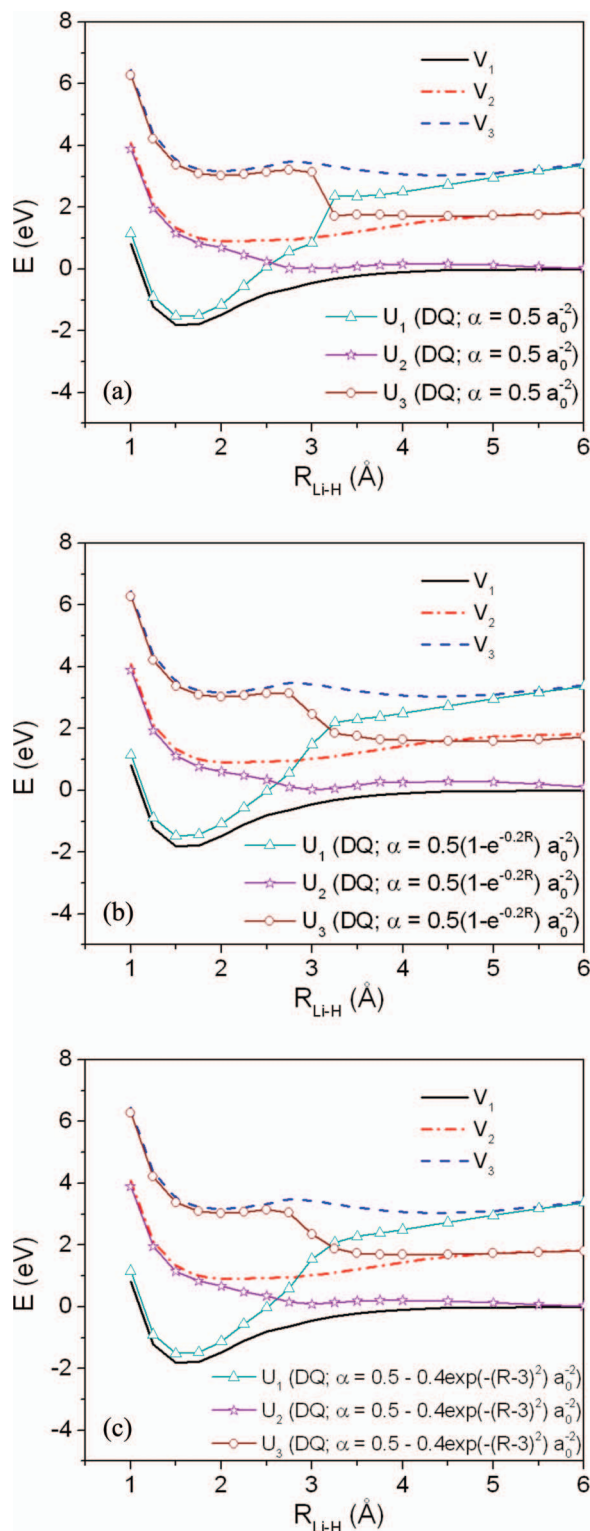


FIG. 2. The adiabatic (V_1 , V_2 , and V_3) and diabatic (U_1 , U_2 , and U_3) potential energy curves of the three lowest-energy $^1\Sigma^+$ states for LiH. The adiabatic states are the same as in Fig. 1, and the diabatic states are obtained by the DQ scheme with (a) $\alpha = 0.5a_0^{-2}$, (b) α given by Eq. (16), and (c) α given by Eq. (17).

the curves less smooth at small Li–H distances. Figure 2(b) agrees with the fourfold way at both small and large Li–H distances by making α a monotonically increasing function,

$$\alpha = A[1 - \exp(-BR_{\text{Li-H}})], \quad (16)$$

TABLE I. The diabatic-state dipole moments (Debye) and the adiabatic and diabatic energies (eV) of LiH obtained by the Boys method, the DQ scheme with two α values, and the threefold way for a Li–H distance of 6.00 Å.^a

	Dipole	Adiabats	Boys	Diabatic energies		
				DQ ($\alpha = 0.1 a_0^{-2}$)	DQ ($\alpha = 0.5 a_0^{-2}$)	Threefold way
State S	0.06	0.00	0.88	0.80	0.03	0.00
State P	0.00	1.82	0.96	1.04	1.81	1.84
State I	28.00	3.40	3.36	3.37	3.37	3.39

^aThe energies are relative to the energy of state S at 20 Å, which is essentially the same as ∞ , where state S is the lowest-energy state.

where $A = 0.5 a_0^{-2}$; $B = 0.2 \text{ \AA}^{-1}$. Figure 2(c) shows even smoother diabatic curves can be obtained by fine adjustment of α , yielding

$$\alpha = A - C \exp[-B(R_{\text{Li-H}} - D)^2], \quad (17)$$

where $A = 0.5 a_0^{-2}$; $B = 1.0 \text{ \AA}^{-2}$; $C = 0.4 a_0^{-2}$; and $D = 3 \text{ \AA}$. We view Figure 2(b) as the best compromise between accuracy and simplicity, and it is encouraging that we get good results with such a simple function because optimization of a nonmonotonic α could be difficult for polyatomics.

Table I shows how well each diabaticization method is able to differentiate between the three states of LiH at 6.00 Å. All methods are capable of separating ionic and covalent states. The Boys localization method is unable to differentiate between the two covalent states, which can be explained by their nearly identical dipole moments. The DQ results are shown for two values of α . With $\alpha = 0.1 a_0^{-2}$, the quadrupole terms are too small to separate the S and P states; however, $\alpha = 0.5 a_0^{-2}$ rectifies this. The DQ method is in very good agreement with the threefold way at this geometry when we use $\alpha = 0.5 a_0^{-2}$.

For U_3 , the threefold way in Figure 1(a) is much smoother than for DQ with any value of α . This is due to the avoided crossing in V_3 near 3 Å. A MO occupied in the dominant CSF of V_3 changes from $2s'$ to $2p_z$ character (the prime indicates that the MO is more diffuse than the one with $2s$ character), which abruptly changes the trace of the quadrupole by a factor of two. This does not noticeably affect the threefold way because MO uniformity is enforced through the threefold-density criterion. The abrupt change in quadrupole near 3 Å also reflects why fitting α to a Gaussian centered at that region gives the best results as shown in Figure 2(c).

The above analysis shows that there are two main deficiencies in Boys localization for LiH. The first is the incorrect dissociation of U_2 and U_3 . The second is the bump in U_1 and U_3 at 2.0 Å. As already mentioned, we do not diagonalize the sub-block of the diabatic Hamiltonian that corresponds to multiple states on the same charge center as suggested in Refs. 25 and 28. This would fix the behavior of U_2 and U_3 near dissociation; however, one is not able to apply this *a posteriori* correction in regions of covalency since at intermediate distances it is not clear where each state is centered. This is the case for LiH at 2.0 Å. We conclude that the Boys

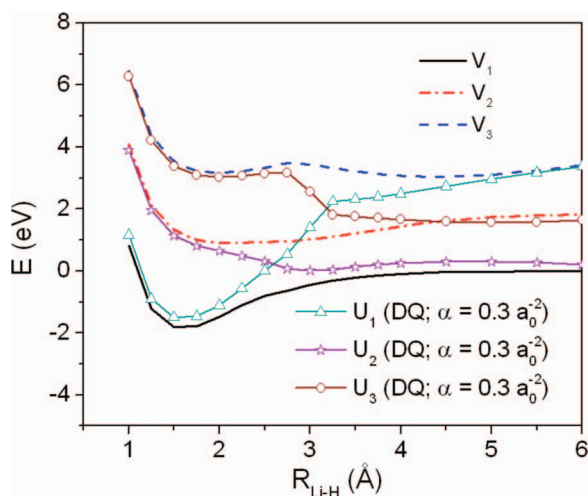


FIG. 3. Same as Fig. 2 except the DQ results are obtained with $\alpha = 0.3 a_0^{-2}$.

localization, while suitable for two-state, two-center electron transfer problems and probably for some more general problems in special cases, is not necessarily an acceptable method for more complex cases, but it also shows that the DQ method is largely able to remove its deficiencies by making the parameter α a function of $R_{\text{Li-H}}$. In fact, results obtained with constant $\alpha = 0.3 a_0^{-2}$ are almost as satisfactory as those obtained with the exponentially increasing α ; this is shown in Figure 3, and Figure 4 compares the best constant α , the best monotonically increasing α obtained with two-parameter exponential function, and the best four-parameter Gaussian function for α . The success of the DQ method with a one-, two-, or four-parameter optimized α is very encouraging because the DQ method is simpler than the threefold or fourfold way in that it does not require an orbital transformation step.

The squared diabatic couplings (U_{ij}^2 where $j = 1, 2,$ and 3 correspond, respectively, to the I, S, and P states of LiH) with (a) the threefold way, (b) Boys localization, and (c) the DQ method are reported in Figure 5. There is no quantitative agreement between the three methods; however, there are similar trends. The Boys method does not yield well-behaved couplings, especially in the crossing regions, where the mag-

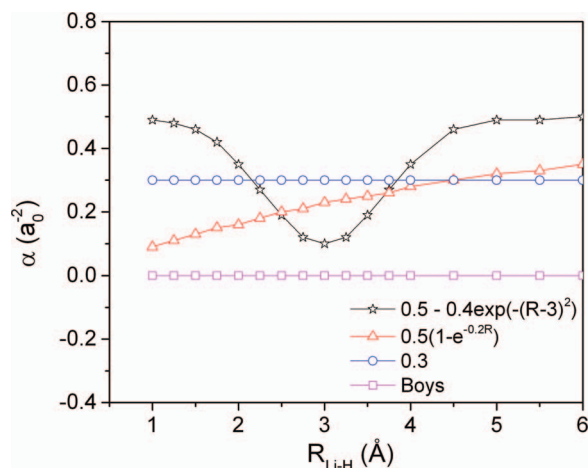


FIG. 4. Forms of α as functions of geometry.

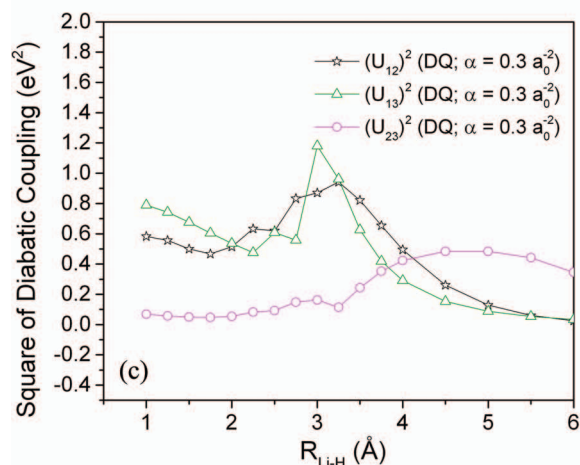
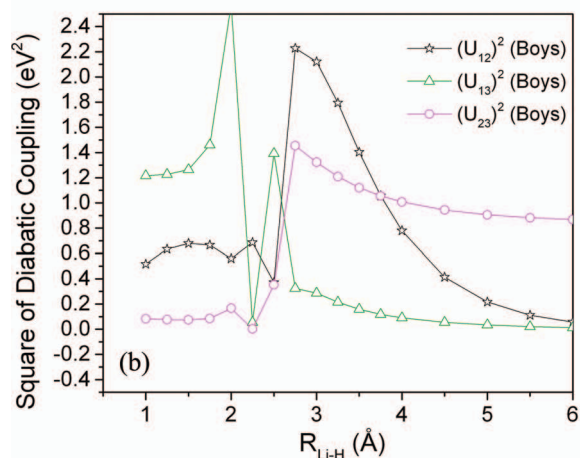
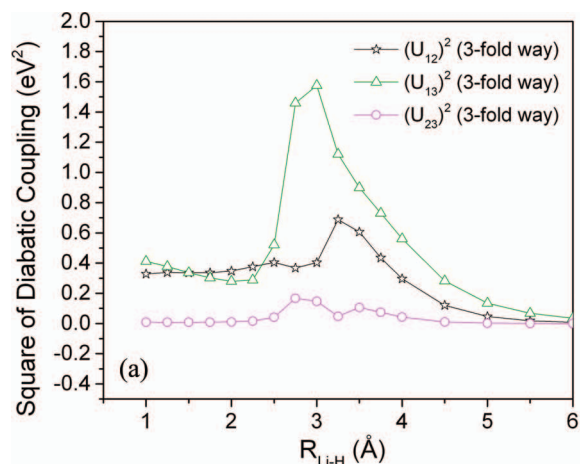


FIG. 5. Squares of the diabatic couplings $[(U_{12})^2, (U_{13})^2,$ and $(U_{23})^2]$ between the three lowest-energy $^1\Sigma^+$ states for LiH. The adiabatic states were computed at the SA(3)-CAS(2,5)SCF/aug-cc-pVTZ level of theory and diabitized with (a) the threefold way, (b) Boys localization, and (c) the DQ method with $\alpha = 0.3a_0^{-2}$.

nitudes are sporadic as shown in Figure 5(b). The large U_{12} and U_{23} coupling are due to the method's inability to separate states S and P at dissociation, which was shown in Figure 1(b). The large U_{13} coupling near 2 Å correlates with the bumps in U_1 and U_3 at 2.0 Å in Figure 1(b). The U_{13} coupling has a sharp peak around 3 Å in the DQ method, which corresponds to the U_1/U_3 crossing in Figures 3. The behavior between 2.0

and 3.0 Å of U_{12} and U_{13} changes noticeably (not shown) as a function α , which correlates to differences in smoothness in this region as shown above. Nevertheless, if we compare our results obtained with the optimum constant value of α (Figure 5(c)) with the threefold way (Figure 5(a)), there are many similarities. The U_{12} coupling has a small local maximum at 2.5 Å for the threefold way and at 2.25 Å for DQ followed by a larger peak at 3.25 Å for the threefold way and at 3 Å for DQ. It is important to note that the trends are shifted by 0.25 Å, which correlates with the shift of 0.25 Å in the potential energy curve crossings in Figures 1(a) and 3. The U_{23} coupling for both methods agrees when $R_{\text{Li-H}}$ is less than 2.5 Å; however, at distances greater than 2.5 Å, the DQ method results in a slowly changing curve while the threefold way U_{23} coupling is a near-zero constant. For the methods unable to properly dissociate LiH (Boys and DQ with $\alpha = 0.1 a_0^{-2}$), U_{23} is far from zero at $R_{\text{LiH}} = 6$ Å, as illustrated for the former in Figure 5(b) (increasing α from 0 to $0.3 a_0^{-2}$ decreases U_{23}^2 from 0.9 eV² to 0.3 eV² at $R_{\text{LiH}} = 6$ Å).

It is certainly not a general expectation that one can always expect the results to be good enough for dynamics calculations, and in fact we expect that there will be cases where the more difficult fourfold way will still be required, but on the systems tested so far, the method has performed well. The disagreement in the U_{23} couplings at small internuclear distances is not considered serious because couplings are mainly important for dynamics in regions close to where the two diabatic states cross; states S and P do not cross. One point to keep in mind here, though, is that variability in coupling in regions where the states are not strongly coupled is not completely unexpected. When the gap between states is large, the results are not sensitive to the precise magnitude of the coupling. This means that the inverse problem of determining the coupling is becoming ill-conditioned, i.e., the couplings are less well determined in the regions where they do not have a large effect.

In Sec. IV.B, we consider a much more difficult problem, the potential energy surfaces for photodissociation of phenol.

IV.B. Phenol

Photodissociation of phenol to phenoxy radical and hydrogen atom is a nonadiabatic process in which the crossings of PESs of three states [$^1\pi\pi$ (S_0), $^1\pi\pi^*$ (S_1), and $^1\pi\sigma^*$ (S_2)] along the O–H fission coordinate play important roles.⁶⁵ At high enough photoexcitation energy, the initially populated bright $^1\pi\pi^*$ state can switch to the dark higher-energy $^1\pi\sigma^*$ state at a crossing or avoided crossing. The system can then follow the repulsive $^1\pi\sigma^*$ state potential energy surface along the hydrogen detachment reaction coordinate to the photo-products of phenoxy radical and hydrogen atom; along the way it passes through a crossing or avoided crossing region with S_0 . Knowledge of the global diabatic PESs and their couplings would allow informative dynamics simulations of this process.^{65(b),65(d),66}

Recently,^{40,67} we have successfully obtained smooth diabatic PESs and couplings for phenol along several important reaction coordinates by using a direct diabatization method based on the fourfold way. Such diabatic calculations for phe-

TABLE II. The dipole moments (Debye) and adiabatic and diabatic energies (eV) obtained by the Boys method, the DQ scheme with two α values, and the fourfold way for the $^1\pi\pi$, $^1\pi\pi^*$, and $^1\pi\sigma^*$ states for a geometry with a C–C–O–H torsion angle of 30° and an O–H distance of 0.964 Å.^a

	Dipole	Adiabats	Boys	Diabats		
				DQ ($\alpha = 1 a_0^{-2}$)	DQ ($\alpha = 10 a_0^{-2}$)	Fourfold way
$^1\pi\pi$	1.63	0.04	2.71	1.47	0.08	0.04
$^1\pi\pi^*$	1.45	5.08	2.43	3.66	5.05	5.08
$^1\pi\sigma^*$	9.93	5.77	5.73	5.74	5.74	5.76

^aThe other geometric parameters are fixed at their values at the planar ground-state equilibrium geometry. The energies are relative energies with respect to the energy of the ground-state equilibrium geometry.

not require great care in constructing the DMOs because the extent of conjugation of the oxygen atom p orbitals to the ring is a sensitive function of the reaction coordinates (which are primarily the O–H fission coordinate and the C–C–O–H torsion coordinate), so that one must carefully define a reference orbital to obtain smooth DMOs, and one must include 2–7 configurations in each dominant CSF list for the diabatic states of interest. By doing this one obtains smooth DMOs, smooth diabatic state functions, and smooth diabatic potentials and couplings.

The diabatization method based on Boys localization²⁸ has its roots in the treatment of charge transfer reactions and does not yield qualitatively correct diabatic states for the photodissociation of phenol. The $^1\pi\pi$ and $^1\pi\pi^*$ states have very similar dipole moments so that the Boys method, being based on dipole moments, has no handle on which to base an adiabatic-to-diabatic transformation. The new DQ diabatization method, by taking account of the traces of the quadrupole tensors in addition to the magnitudes of the dipole vectors, so that one takes account of higher-order characteristics of the charge distributions as well as their first moments, provides a convenient and straightforward method of broader applicability, and here we test it for phenol.

Table II lists the adiabatic energies and diabatic energies of the $^1\pi\pi$, $^1\pi\pi^*$, and $^1\pi\sigma^*$ states, obtained by the Boys, DQ, and fourfold way methods, for a geometry with C–C–O–H torsion angle (τ) of 30°, in which the other internal coordinates are fixed at their values at the ground-state equilibrium geometry—in particular the O–H distance ($R_{\text{O-H}}$) is 0.964 Å. The energies in the table are relative to the energy of the planar ground-state equilibrium geometry of phenol. For the equilibrium value of $R_{\text{O-H}}$, the three states are well separated, and their diabats are very similar to their diabats. However, because of the similar dipoles of the $^1\pi\pi$ and $^1\pi\pi^*$ states, Boys localization diabatization cannot distinguish the two states. Table II shows that the DQ method with $\alpha = 1 a_0^{-2}$ improves the diabats, and with $\alpha = 10 a_0^{-2}$ it reproduces the diabatic PESs of the three involved states obtained by the fourfold way.

Figures 6 and 7 present results as functions of the O–H distance, $R_{\text{O-H}}$, with the C–C–O–H torsion angle, τ , equal to 30° and the other internal coordinates fixed at their values at the planar ground-state equilibrium geometry. The

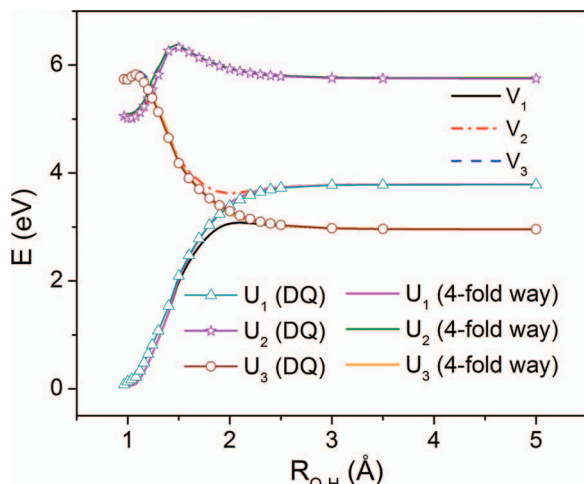


FIG. 6. Adiabatic (V_1 , V_2 , and V_3) and diabatic (U_1 , U_2 , and U_3) potential energy surfaces along $R_{\text{O-H}}$ coordinate of phenol at C–C–O–H torsion angle of 30° , with the other internal coordinates fixed at the ground-state equilibrium geometry. The energies are relative to the energy of the planar ground-state equilibrium geometry. The DQ calculations are carried out using $\alpha = 10 a_0^{-2}$.

diabatic and adiabatic PESs (U_j and V_j , respectively, for $j = 1-3$) are shown in Fig. 6, and the squares of the diabatic couplings (U_{jj}^2) are in Fig. 7. For O–H distances shorter than 1.44 \AA , the three diabatic surfaces have the following character: U_1 is $^1\pi\pi$, U_2 is $^1\pi\pi^*$, and U_3 is $^1\pi\sigma^*$; however, at $R_{\text{O-H}} = 1.44 \text{ \AA}$, due to another crossing with a higher energy $^1\pi\sigma^*$ state, the U_2 surface starts to represent that higher energy $2^1\pi\sigma^*$ state and has $^1\pi\sigma^*$ character for larger $R_{\text{O-H}}$. Figure 6 shows that the diabatic PESs obtained by the DQ method with $\alpha = 10 a_0^{-2}$ agree very well with those obtained by the fourfold way. Figure 7 shows that the DQ method always overestimates the couplings compared to fourfold way, especially for $R_{\text{O-H}} < 1.50 \text{ \AA}$, where the DQ U_{12} and U_{13} couplings are significantly larger than the fourfold way ones, but we should keep in mind that the diabatic couplings are significant for the dynamics mainly when the surfaces are strongly

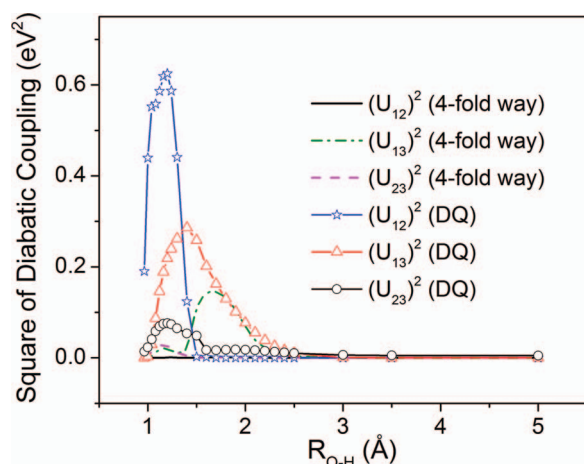


FIG. 7. Squares of the diabatic couplings [$(U_{12})^2$, $(U_{13})^2$, and $(U_{23})^2$] along the O–H bond stretching coordinate of phenol at a C–C–O–H torsion angle of 30° , with the other internal coordinates fixed at the ground-state equilibrium geometry. The DQ calculations were carried out with $\alpha = 10 a_0^{-2}$.

interacting. For $R_{\text{O-H}} < 1.50 \text{ \AA}$, the U_1 and U_2 surfaces are well separated, as are the U_1 and U_3 surfaces, and the overestimations of U_{12} and U_{13} couplings may have little influence on the dynamics simulations. The U_{13} couplings obtained by two methods agree well in the strong interaction region ($R_{\text{O-H}} = 1.70\text{--}2.20 \text{ \AA}$) of the U_1 and U_3 surfaces. The U_{23} couplings obtained by DQ method are about twice as large as those in the fourfold way around the crossing region ($R_{\text{O-H}} = 1.10\text{--}1.30 \text{ \AA}$) of the U_2 and U_3 curves, but they have similar trends, and the values are still reasonable. Due to the high-energy crossing of the third and fourth PESs, there is a small bump in the $(U_{23})^2$ curves for $R_{\text{O-H}} = 1.50 \text{ \AA}$. This bump would not affect the photodissociation dynamics very much because it happens in the weak interaction region of the U_2 and U_3 surfaces where the U_{23} coupling is not important. Therefore, the results presented here indicate that the DQ method with $\alpha = 10 a_0^{-2}$ provides a suitable diabaticization method for simulating the photodissociation of phenol.

V. CONCLUSION

In this paper, we have presented a new diabaticization method, called the DQ method, that uses the magnitude of the dipole vector and the trace of the quadrupole tensor to transform adiabatic states to diabatic states. It is a straightforward scheme, applicable with any electronic structure method and not restricted to two-state problems or electron transfer systems. We applied this method to two cases: LiH and phenol.

The results for LiH show that a constant value for the single parameter α can give much better results than Boys localization, and a two-parameter exponentially increasing function for α can give results almost as good as those obtained by the threefold way (the fourfold way reduces to the threefold way for LiH). Our results for phenol are very encouraging because we obtain very comparable results with the fourfold way and DQ. In such a case, the DQ method has real advantages because it does not require specifying reference orbitals and making orbital transformations.

A very attractive feature of the DQ method is its ease of application; no orbital transformations are required, and the information required from electronic structure calculations at a given geometry would fit on the back of an envelope: N adiabatic energies, the $N \times N$ dipole transition matrix, and the $N \times N$ transition matrix of the sum of the diagonal elements of the primitive quadruple (for a specific origin of the coordinate system, but independent of the orientation of the axes; note that both $N \times N$ transition matrices are symmetric, so for $N = 3$, this amounts to 15 numbers). Therefore, the method can be applied with any electronic structure method for which these matrices are available. One of our objectives for a diabaticization method is that it should be able to treat general reactions, not just two-state, electron transfer reactions, whereas the dipole method should not be expected to be useful for cases where the states do not differ by charge transfer. The phenol test case is therefore an important challenge. The success of the DQ method, coupled to the ease of application of the DQ method, is very encouraging.

ACKNOWLEDGMENTS

This work was supported by the Scientific Discovery through Advanced Computing (SciDAC) program funded by U.S. Department of Energy, Office of Science, Basic Energy Sciences and Advanced Scientific Computing Research under Award No. DE-SC0008666.

APPENDIX: EQUIVALENCE OF BOYS FORMULATIONS

There is more than one formulation of the Boys localization method for MOs.^{45,46,71} This appendix shows that two formulations that are equivalent for MOs are analogously equivalent for many-electron states. Let us begin by rewriting Eq. (5) as

$$\begin{aligned} f_{Boys} &= \sum_{A,B} |\langle \phi_A | \boldsymbol{\mu} | \phi_A \rangle - \langle \phi_B | \boldsymbol{\mu} | \phi_B \rangle|^2 \\ &= \sum_{A,B} |\langle \phi_A | \boldsymbol{\mu} | \phi_A \rangle|^2 + |\langle \phi_B | \boldsymbol{\mu} | \phi_B \rangle|^2 \\ &\quad - 2 \langle \phi_A | \boldsymbol{\mu} | \phi_A \rangle \cdot \langle \phi_B | \boldsymbol{\mu} | \phi_B \rangle \\ &\propto \sum_A |\langle \phi_A | \boldsymbol{\mu} | \phi_A \rangle|^2 - \left| \sum_A \langle \phi_A | \boldsymbol{\mu} | \phi_A \rangle \right|^2. \quad (\text{A1}) \end{aligned}$$

The second term in the last expression is the square of the trace of a matrix. Because the trace of a matrix is invariant to unitary transformations, the second term will have no effect on the function during maximization. Thus,

$$f_{Boys} \propto \sum_A |\langle \phi_A | \boldsymbol{\mu} | \phi_A \rangle|^2. \quad (\text{A2})$$

- ¹C. A. Mead and D. G. Truhlar, *J. Chem. Phys.* **77**, 6090 (1982).
- ²B. C. Garrett and D. G. Truhlar, in *Theoretical Chemistry: Theory of Scattering: Papers in Honor of Henry Eyring*, edited by D. Henderson (Academic, New York, 1981), pp. 215–289.
- ³D. R. Bates, H. S. W. Massey, and A. L. Stewart, *Proc. R. Soc. London* **A216**, 437–458 (1953).
- ⁴C. F. Melius and W. A. Goddard III, *Phys. Rev. A* **10**, 1541–1557 (1974).
- ⁵B. C. Garrett, D. G. Truhlar, and C. F. Melius, in *Energy Storage and Redistribution in Molecules*, edited by J. Hinze (Plenum Press, New York, 1983), pp. 375–395.
- ⁶D. R. Bates and R. McCarroll, *Proc. R. Soc. London* **A245**, 175–183 (1958).
- ⁷A. W. Jasper, B. K. Kendrick, C. A. Mead, and D. G. Truhlar, in *Modern Trends in Chemical Reaction Dynamics: Experiment and Theory (Part I)*, edited by X. Yang and K. Liu (World Scientific, Singapore, 2004), pp. 329–391.
- ⁸A. Macias and A. Riera, *J. Phys. B* **11**, L489 (1978).
- ⁹F. Spiegelmann and J. P. Malrieu, *J. Phys. B* **17**, 1259 (1984).
- ¹⁰R. Cimbriglia, in *Time-Dependent Quantum Molecular Dynamics*, edited by J. Broeckhove and L. Lathouwers (Plenum, New York, 1992), pp. 11–26.
- ¹¹K. Ruedenberg and G. J. Atchity, *J. Chem. Phys.* **99**, 3799 (1993).
- ¹²G. J. Atchity and K. Ruedenberg, *Theor. Chem. Acc.* **97**, 47 (1997).
- ¹³E. S. Kryachenko and D. R. Yarkony, *Int. J. Quantum Chem.* **76**, 235 (2000).
- ¹⁴M. P. Filscher and L. Serrano-Andrés, *Mol. Phys.* **100**, 903 (2002).
- ¹⁵H. Nakamura and D. G. Truhlar, *J. Chem. Phys.* **115**, 10353 (2001).
- ¹⁶H. Nakamura and D. G. Truhlar, *J. Chem. Phys.* **117**, 5576 (2002).
- ¹⁷H. Nakamura and D. G. Truhlar, *J. Chem. Phys.* **118**, 6816 (2003).
- ¹⁸K. R. Yang, X. Xu, and D. G. Truhlar, *Chem. Phys. Lett.* **573**, 84 (2013).
- ¹⁹R. Thürwächter and P. Halvick, *Chem. Phys.* **221**, 33 (1997).
- ²⁰W. Domcke and C. Woywood, *Chem. Phys. Lett.* **216**, 362 (1993).
- ²¹D. Simah, B. Hartke, and H.-J. Werner, *J. Chem. Phys.* **111**, 4523 (1999).
- ²²R. Mulliken, *J. Am. Chem. Soc.* **74**, 811 (1952).

- ²³N. Hush, *Prog. Inorg. Chem.* **8**, 391 (1967).
- ²⁴H.-J. Werner and W. Meyer, *J. Chem. Phys.* **74**, 5802 (1981).
- ²⁵R. J. Cave and M. D. Newton, *Chem. Phys. Lett.* **249**, 15 (1996).
- ²⁶A. A. Voityuk and N. Rosch, *J. Chem. Phys.* **117**, 5607 (2002).
- ²⁷Q. Wu and T. Van Voorhis, *J. Chem. Theory Comput.* **2**, 765 (2006).
- ²⁸J. E. Subotnik, S. Yeganeh, R. J. Cave, and M. A. Ratner, *J. Chem. Phys.* **129**, 244101 (2008).
- ²⁹J. E. Subotnik, R. J. Cave, R. P. Steele, and N. Shenvi, *J. Chem. Phys.* **130**, 234102 (2009).
- ³⁰C. P. Hsu, *Acc. Chem. Res.* **42**, 509 (2009).
- ³¹J. E. Subotnik, J. Vura-Weis, A. J. Sodt, and M. A. Ratner, *J. Phys. Chem. A* **114**, 8665 (2010).
- ³²B. O. Roos, P. R. Taylor, and P. E. M. Siegbahn, *Chem. Phys.* **48**, 157 (1980).
- ³³H. Nakano, *J. Chem. Phys.* **99**, 7983 (1993).
- ³⁴R. Valero and D. G. Truhlar, *J. Chem. Phys.* **125**, 194305 (2006).
- ³⁵Z. H. Li, R. Valero, and D. G. Truhlar, *Theor. Chem. Acc.* **118**, 9 (2007).
- ³⁶R. Valero and D. G. Truhlar, *J. Phys. Chem. A* **111**, 8536 (2007).
- ³⁷R. Valero, D. G. Truhlar, and A. W. Jasper, *J. Phys. Chem. A* **112**, 5756 (2008).
- ³⁸R. Valero, L. Song, J. Gao, and D. G. Truhlar, *J. Chem. Theory Comput.* **5**, 1 (2009).
- ³⁹R. Valero and D. G. Truhlar, *J. Chem. Phys.* **137**, 22A539 (2012).
- ⁴⁰X. Xu, K. R. Yang, and D. G. Truhlar, *J. Chem. Theory Comput.* **9**, 3612 (2013).
- ⁴¹In Ref. 15, the authors approximated $\xi_i(\mathbf{R}^{\text{Ref}})|\xi_j(\mathbf{R})$ as $\xi_i(\mathbf{R})|\xi_j(\mathbf{R})$.
- ⁴²B. O. Roos, in *Theory and Applications of Computational Chemistry: The First Forty Years*, edited by C. E. Dykstra, G. Frenking, K. S. Kim, and G. E. Scuseria (Elsevier, Amsterdam, 2005), pp. 725–764.
- ⁴³M. W. Schmidt and M. S. Gordon, *Annu. Rev. Phys. Chem.* **49**, 233 (1998).
- ⁴⁴R. N. Diffenderfer and D. R. Yarkony, *J. Phys. Chem.* **86**, 5098 (1982).
- ⁴⁵J. M. Foster and S. F. Boys, *Rev. Mod. Phys.* **32**, 300 (1960).
- ⁴⁶C. Edmiston and K. Ruedenberg, *Rev. Mod. Phys.* **35**, 457 (1963).
- ⁴⁷E. Alguire and J. E. Subotnik, *J. Chem. Phys.* **135**, 044114 (2011).
- ⁴⁸Q. Ou and J. E. Subotnik, *J. Phys. Chem. C* **117**, 19839 (2013).
- ⁴⁹X. Liu and J. E. Subotnik, *J. Chem. Theory Comput.* **10**, 1004 (2014).
- ⁵⁰H.-J. Werner and W. Meyer, *J. Chem. Phys.* **74**, 5794 (1981).
- ⁵¹P. T. Eubank, *AIChE J.* **18**, 454 (1972).
- ⁵²A. D. Buckingham, *Q. Rev.* **13**, 183 (1959).
- ⁵³M. J. Gunning and R. E. Raab, *Mol. Phys.* **91**, 589 (1997).
- ⁵⁴A. J. Cohen and Y. Tantirungrotechai, *Chem. Phys. Lett.* **299**, 465 (1999).
- ⁵⁵S. Höfner and M. Wendland, *Int. J. Quantum Chem.* **86**, 199 (2002).
- ⁵⁶D. A. Kleier, T. A. Halgren, J. H. Hall, and W. N. Lipscomb, *J. Chem. Phys.* **61**, 3905 (1974).
- ⁵⁷F. Aquilante, L. De Vico, N. Ferré, G. Ghigo, P.-Å. Malmqvist, P. Neogrády, T. B. Pedersen, M. Pitoňák, M. Reiher, B. O. Roos, L. Serrano-Andrés, M. Urban, V. Velyazov, and R. Lindh, *J. Comput. Chem.* **31**, 224 (2010).
- ⁵⁸P.-Å. Malmqvist, *Int. J. Quantum Chem.* **30**, 479 (1986); P.-Å. Malmqvist and B. O. Roos, *Chem. Phys. Lett.* **155**, 189 (1989).
- ⁵⁹D. R. Bates and T. J. M. Boyd, *Proc. Phys. Soc. London, Ser. A* **69**, 910 (1956).
- ⁶⁰R. Grice and D. R. Herschbach, *Mol. Phys.* **27**, 159 (1974).
- ⁶¹R. W. Numrich and D. G. Truhlar, *J. Phys. Chem.* **79**, 2745 (1975).
- ⁶²J. J. Camacho, J. M. L. Poyato, A. Pardo, and D. Reyman, *J. Chem. Phys.* **109**, 9372 (1998).
- ⁶³N. Khelifi, *Phys. Rev. A* **83**, 042502 (2011).
- ⁶⁴M. S. Gordon and M. W. Schmidt, in *Theory and Applications of Computational Chemistry: The First Forty Years*, edited by C. E. Dykstra, G. Frenking, K. S. Kim, and G. E. Scuseria (Amsterdam, 2005), p. 1167.
- ⁶⁵(a) A. L. Sobolewski, W. Domcke, C. Dedonder-Lardeux, and C. Jourvet, *Phys. Chem. Chem. Phys.* **4**, 1093 (2002); (b) Z. Lan, W. Domcke, V. Vallet, A. L. Sobolewski, and S. Mahapatra, *J. Chem. Phys.* **122**, 224315 (2005); (c) M. N. R. Ashfold, B. C. Cronin, A. L. Devine, R. N. Dixon, and M. G. D. Nix, *Science* **312**, 1637 (2006); (d) O. P. J. Vieuxmaire, Z. Lan, A. L. Sobolewski, and W. Domcke, *J. Chem. Phys.* **129**, 224307 (2008); (e) M. N. R. Ashfold, A. L. Devine, R. N. Dixon, G. A. King, M. G. D. Nix, and T. A. A. Oliver, *Proc. Natl. Acad. Sci. U.S.A.* **105**, 12701 (2008); (f) R. N. Dixon, T. A. A. Oliver, and M. N. R. Ashfold, *J. Chem. Phys.* **134**, 194303 (2011).
- ⁶⁶(a) S. G. Ramesh and W. Domcke, *Faraday Discuss.* **163**, 73 (2013); (b) X. Zhu and D. R. Yarkony, *J. Chem. Phys.* **140**, 024112 (2014).
- ⁶⁷K. R. Yang, X. Xu, J. Zheng, and D. G. Truhlar, “Full-dimensional potentials and state couplings and multidimensional tunneling calculations for the photodissociation of phenol,” *Chemical Science* (published online).

- ⁶⁸(a) T. H. Dunning, *J. Chem. Phys.* **90**, 1007 (1989); (b) R. A. Kendall, T. H. Dunning, and R. J. Harrison, *ibid.* **96**, 6796 (1992).
- ⁶⁹(a) E. Papajak, H. R. Leverentz, J. Zheng, and D. G. Truhlar, *J. Chem. Theory Comput.* **5**, 1197 (2009); (b) **5**, 3330 (2009); (c) E. Papajak and D. G. Truhlar, *ibid.* **7**, 10 (2011).
- ⁷⁰H. Nakamura, J. D. Xidos, A. C. Chamberlin, C. P. Kelly, R. Valero, K. R. Yang, J. D. Thompson, J. Li, G. D. Hawkins, T. Zhu, B. J. Lynch, Y. Volobuev, D. Rinaldi, D. A. Liotard, C. J. Cramer, and D. G. Truhlar, *Hondoplus-v5.2* (University of Minnesota, Minneapolis, MN, 2013); M. Dupuis, A. Marquez, and E. R. Davidson, *Hondo 99.6* (Pacific Northwest National Laboratory, Richland, WA, 1999); M. Dupuis, A. Marquez, and E. R. Davidson, *Hondo95.3, Quantum Chemistry Program Exchange (QCPE)* (Indiana University, Bloomington, IN, 2005).
- ⁷¹S. F. Boys, in *Quantum Theory of Atoms, Molecules, and the Solid State*, edited by P. Löwdin (Academic, New York, 1966), p. 253.